Eur. Phys. J. B **8**, 143–149 (1999)

THE EUROPEAN PHYSICAL JOURNAL B

EDP Sciences

On the Mössbauer studies of harmonically bound quantum oscillators in Brownian motion

A. Razdan[a]

Bhabha Atomic Reseach Centre, Nuclear Research Laboratory, Trombay, Bombay 400 085, India

Received 16 July 1997 and Received in final form 2 September 1998

Abstract. In many biological systems like whole cells, membranes or proteins and some of the polymeric systems, dynamics reveals itself in Mössbauer spectra as a non Lorentzian behaviour above some particular temperature which is characteristic of the system. Moreover mean square displacement and line width show temperature dependence above the characteristic temperature. Brownian motion of harmonically bound oscillator has been able to explain the non-Lorentzian behaviour. In the present paper, a quantum picture of the above model is discussed and lineshape is expressed as the closed form for the extreme overdamping case. In addition to the non-Lorentzian behaviour, the present model also predicts a temperature dependence of mean square displacement and linewidth.

PACS. 87.10.+e General, theoretical, and mathematical biophysics (including logic of biosystems, quantum biology, and relevant aspects of thermodynamics, information theory, cybernetics, and bionics) – 76.20.+q General theory of resonances and relaxations – 76.80.+y Mössbauer effect; other-ray spectroscopy

1 Introduction

Mössbauer absorption spectra of various biological systems such as proteins, membranes and whole cells and some polymeric systems show unusual features [1–9]. It is observed that (i) above a certain temperature which is characteristic of the system, the spectrum exhibits a second broad line besides the usual narrow line at the same frequency, (ii) f-factor (recoilless fraction) shows a temperature dependence which is not typical of the Einstein or the Debye model and (iii) the width of the lineshape increases with the temperature.

In addition to the Mössbauer spectroscopy, protein dynamics is being studied by the Nuclear Magnetic Resonance (NMR) [10], Neutron scattering [11], X-ray dynamical analysis and, more recently, by the RSMR (Rayleigh Scattering of Mössbauer Radiations). By using RSMR, some interesting results have been reported [12,13,28] which are consistent with the Mössbauer results.

Two extreme theoretical models of bounded diffusion have been used to analyse the results, one is of discrete [3] and the other is of continuous nature [15]. In the former, it is assumed that an atom can jump stochastically between finite number of fixed points with a constant jump probability per unit time. The continuous case is based on the assumption that the particle is bound in a three-dimensional well and whose motion is overdamped by strong frictional forces. It is observed that within a certain range of parameters D (diffusion constant) and α (ratio of the harmonic force constant to the damping force constant), the spectrum is made up of a narrow line and a wide component and fits well the experimentally observed spectra. Nowik *et al.* [16] have considered a generalised case of continuous diffusion and discussed the extreme underdamped case in addition to the extreme overdamped case and expressed the respective lineshapes in closed form. It may be noted that in both the jump and continuous diffusion models, the total area under the Mössbauer lineshapes remains unaffected by diffusive motion [14,16]. Thus, the appearance of the diffusive motion above the critical temperature should not affect the temperature dependence of f (recoilless fraction). However, experimentally it has been observed that above the critical temperature, f shows an additional temperature dependence [17] and area under the Mössbauer lineshape does not remain constant. Hence, in both of the models, described above, besides assuming diffusive motion, one has to assume an additional degree of freedom to account for the temperature dependence of f. An attempt has been made to understand the temperature dependence of the mean square displacement in terms of extending the Brownian motion oscillator model [18,19].

In the present, paper, quantum picture of the harmonically bound oscillator in Brownian motion has been discussed and line shape is expressed in the closed form for extreme overdamped case. The calculations are based on the assumption that the unfrozen conformational states may be represented in terms of overdamped quantum

[a] e-mail: akradzan@apsara.barc.ernet.in

oscillators acted upon by random force. It is worth mentioning here that the quantum picture has already been considered for such problems as Afanseev and Sedov [27] treated the problem of diffusion by introducing an operator called "relaxational operator" and reduced the problem to a solution of Schrodinger equation for a given potential. After making the "relaxational operator" Hermitian, it becomes the Hamiltonian operator describing the motion of a quantum particle for a given potential. But theoretically predicted MSD *versus* temperature curves predicted by Afanseev and Sedov [27] do not agree with experimentally observed behaviour.

2 Lineshape using classical correlation function

Presence of diffusive motions in biological systems was first reported by Cohen *et al.* [1] in oxygen binding protein, myoglobin, in two of its forms, metmyoglobin and deoxymyoglobin and in Ferritin, a crystal of iron storage proteins. Similar phenomena has been observed in haemoglobin by Mayo, Parak and Mössbauer [3]. Pioneering studies on the use of Mössbauer absorption spectroscopy has been done by Keller and Debrunner for oxymyoglobin in frozen solutions [17], Parak, Prolov, Mössbauer and Glodanskii [30] on the crystals of metmyoglobin. In all these systems, lineshape was non-Lorentzian above some particular temperature (system dependent) and other features like sharp fall in the recoil-free fraction and increase of linewidth with temperature have also been reported.

Singwi and Sjolander [31] were first to predict the possibility of diffusion studies by Mössbauer spectroscopy and obtained a general formula for Mössbauer spectrum in terms of classical self correlation function. For one dimensional harmonic oscillator in Brownian motion Ulhenbeck and Ornstein [32] derived a general formula for self correlation function $G(x, x_0, t)$, which is the probability that at time t, nucleus will be at position x if at time zero it was at position x_0. Nowik *et al.* [15,16] generalized this self correlation function to three dimensions for the overdamped case with the condition $\lambda t \gg 1$ (λ = damping constant) and obtained a simple formula for Mössbauer lineshape which is given as

$$I(\omega) = \frac{1}{2\pi}\int_{-\infty}^{\infty} dt \exp\left[-i(\omega-\omega_0)t - \frac{1}{2}\Gamma|t|\right] - \left(\frac{k^2 D}{\alpha}\right)(1-\exp(-\alpha|t|)) \quad (1a)$$

where $\alpha = \frac{w^2}{\lambda}$, w is the harmonic force constant. Nowik *et al.* were able to explain non-Lorentzian behaviour of biological systems using equation (1a) by varying parameter α, which is the ratio of harmonic force constant to the damping force constant. Here it is important to note that Gunther *et al.* [33] were first to argue that Mössbauer effect can used as an experimental tool to study Brownian motion. Again Gunther *et al.* [34] were first to predict that Brownian motion of Mössbauer atom results in non-Lorentzian nature of Mössbauer lineshape.

3 Lineshape using quantum correlation function

The present paper is essentially quantum version of Nowik *et al.* paper [16]. In this paper, we show that quantum picture not only explains non-Lorentzian behaviour but also fits well to the temperature dependence of mean square displacement and linewidth, which is not possible from classical approach.

Agarwal developed the quantum version of Ulhenbeck and Orstein theory [21] by using phase space distribution function. Dattagupta [12] considered the Brownian motion of the quantum system and derived the master equation. Self-correlation function in quantum case is defined as [23]

$$G(k,t) = \langle \exp[-ikx(t)]\exp[ikx(0)]\rangle \quad (1b)$$

where $x(0)$ is the position operator of the nucleus at time zero and $x(t)$ is its Heisenberg form at time t. Duttagupta and Reiter [23] used Agarwal 's formalism to derive self correlation for the quantum oscillator in the Brownian motion. we use this quantum correlation function and for the overdamped case with $\lambda \gg w$, $\lambda t \gg 1$, self correlation function is given as

$$G(k,t) = \exp[-D(t)\ k^2] \quad (1c)$$

where

$$D(t) = (\hbar/2mw_2)\sinh w_2 t \exp(-\lambda t) + (\hbar\eta/mw_2) \times [1-\exp(-\lambda t)](\cosh w_2 t + (\lambda/w_2)\sinh w_2 t) \quad (2)$$

when $w_2^2 = \lambda^2 - w^2 > 0$

For the overdamped case with $\lambda \gg w, \lambda t \gg 1$ and

$$\eta = [\exp(\beta\hbar w_2) - 1]^{-1}. \quad (3)$$

Following the approach of Nowik *et al.* [16], the second term of $D(t)$, after simplification, turns out to be equal to

$$\frac{\hbar\eta}{mw_2}\left[1-\exp\left(\frac{w_2^2}{2\lambda} - t\right)\right]$$

so that

$$\begin{aligned} D(t) &= \left(\frac{\hbar}{2mw_2}\right)\sinh(w_2 t)\exp(-\lambda t) + \left(\frac{h\eta}{mw_2}\right) \\ &\quad \times \left[1-\exp\left(-\frac{w_2^2}{2\lambda}t\right)\right] \\ &= \frac{\hbar}{2mw_2}\left[\frac{e^{(w_2-\lambda)t} - e^{-(w_2+\lambda)t}}{2}\right] \\ &\quad + \frac{h\eta}{mw_2}\left[1-\exp\left(-\frac{w^2}{2\lambda}t\right)\right]. \end{aligned}$$

Now $w_2 = (\lambda^2 - w^2)^{1/2} = \lambda - \frac{w^2}{2\lambda}$, $w_2 - \lambda = -\frac{w^2}{2\lambda}$.

Also $w_2 \approx \lambda$.

Hence

$$D(t) = \left(\frac{\hbar}{2mw_2}\right)\left[\frac{e^{(-w^2/2\lambda t)}}{2} - \frac{e^{-2\lambda t}}{2}\right] + \frac{\hbar\eta}{mw_2}\left[1 - \exp\left(-\frac{w^2}{2\lambda}t\right)\right].$$

Since $\lambda t \gg 1$, $\exp(-2\lambda t)$ can be neglected. Let $\alpha = w^2/2\lambda$, we have

$$D(t) = \frac{\hbar\eta}{mw_2} + \left[\left(\frac{\hbar}{4mw_2} - \frac{\hbar\eta}{mw_2}\right)\ \exp(-\alpha \mid t \mid)\right]. \quad (4)$$

The Mössbauer lineshape can be written as

$$I(\omega) = \frac{1}{2\pi}\int_{-\infty}^{\infty} dt\ \exp[-i(\omega-\omega_o)t - 1/2\Gamma \mid t \mid] \times \exp[-D(t)k^2]. \quad (5)$$

For the extreme case of overdamping, the lineshape in the closed form is given by

$$I(\omega) = \exp\left(-k^2\langle x\rangle_q^2\right)\left[\sum_{n=0}^{\infty}\frac{1}{n!}\left(\frac{\hbar k^2\eta}{mw_2} - \frac{\hbar k^2}{4mw_2}\right)^n \frac{(\Gamma/2 + n\alpha)/\pi}{((\Gamma/2+n\alpha)^2 + (\omega-\omega_o)^2}\right] \quad (6)$$

where $\langle x\rangle_q^2 = \hbar\eta/mw_2$.

It is evident from $I(\omega)$ that area under the curve does not remain constant. In some systems like single crystal proteins or oriented membranes [16], Mössbauer spectra may have contributions due to anisotropic diffusive motions. For such cases, one has to consider independent motions along these axes. Hence, for an anisotropic overdamped harmonic oscillator, with independent motions along the three axes, equation (6) can be rewritten as

$$I(w) = \frac{1}{2\pi}\int_{-\infty}^{\infty} dt\ \exp[-i(\omega-\omega_o)t - 1/2\Gamma \mid t \mid \times \exp\left[\Sigma_{j=x,y,z} - D_j(t)k_j^2\right] \quad (7)$$

where

$$D_j(t) = \frac{\hbar\eta}{mw_{2j}} + \left[\left(\frac{\hbar}{4mw_{2j}} - \frac{h\eta}{mw_{2j}}\right)\exp\left(-\alpha_j \mid t \mid\right)\right] \quad (8)$$

with $\alpha_j = w_{2j}^2/\lambda_j$, $(j = x, y, z)$.

The lineshape for polycrystalline samples result due to various transitions between various substates. In the case of overdamped harmonic oscillators for the Einstein Model of a solid, the Mössbauer lineshape in presence of the quadrupole interaction is given as

$$I(\omega) = \frac{1}{8\pi^2}\int_{\phi}\int_{\theta}\int_{-\infty}^{\infty} dt\left[\exp -i(\omega-\omega_o)t - \Gamma/2 \mid t \mid\right] \times \exp\left[-D_x(t)k^2\cos^2\theta - k^2\sin^2\theta\left[\cos^2\phi\ D_y(t) + \sin^2\phi\ D_z(t)\right]\right] f(\Delta m, \theta)\ \sin\theta\ d\theta\ d\phi \quad (9)$$

where D_x, D_y and D_z are given by equation (8). Equation (9) is essentially the spectral shape of a nuclear transition taking place between the quantum numbers M_1 and M_2 with $M_1 - M_2 = \Delta m$, for a powder sample in presence of the Karyagin-Goldanskii effect. $f(\Delta m, \theta)$ for the transition ^{57}Fe is given by $f(0,\theta) = (3/2)\sin^2\theta$ and $f(\pm 1, \theta) = (3/4)(1+\cos^2\theta)$. For the axial symmetry, $\langle z^2\rangle = \langle y^2\rangle$ and $\mu = \cos\theta$. In this case, equation (9) can be written as

$$I(\omega) = \frac{1}{2\pi}\int_{-\infty}^{\infty} dt\int_0^1 \exp[-i(\omega-\omega_o)t - 1/2\Gamma \mid t \mid] \times \exp[-k^2 D_x(t)\mu^2 - k^2 D_y(t)(1-\mu^2)] f_s(\mu) d\mu \quad (10)$$

where $f_1(\mu) = \frac{3}{4}(1+\mu^2)$ and $f_2(\mu) = \frac{3}{4}\left(\frac{5}{3} - \mu^2\right)$.

This theoretical treatment holds for the case when all oscillators have the same frequency, *i.e.*, Einstein's Model. For Debye Model, one has to consider a distribution of frequencies.In order to derive generalized lineshape, we express the displacement r of the nucleus for the systems like proteins and polymers, in terms of normal coordinates q_l [16] where $l = 1, 2, ..., N$. If the wave vector of the γ-ray is $\mathbf{k} = k\epsilon$ we can write [16]

$$(\mathbf{k}.r) = \mathbf{k}(\epsilon.\mathbf{r}) = k\sum_l a_l q_l. \quad (11)$$

Assuming that all the normal-modes coordinates follow the harmonic motion and if in all the cases overdamped limit holds, and since all normal modes are statistically uncorrelated [16] hence the lineshape can be written as

$$I(\omega) = \frac{1}{2\pi}\int_{-\infty}^{\infty} dt\ \exp[-i(\omega-\omega_o)t - 1/2\Gamma \mid t \mid] \times \exp\left[-\sum_{l=1}^{N} D_l(t)a_l^2k^2\right] \quad (12)$$

where

$$D_1(t) = \frac{\hbar\eta}{mw_{2l}} + \left[\frac{\hbar}{4mw_{2l}} - \frac{\eta\hbar}{mw_{2l}}\right]\exp(-\alpha_l \mid t \mid)$$

and $\alpha_l = w_l^2/2\lambda_l$.

Out of N possible modes there may be, say, j modes for which $\omega_j^2/\lambda_j \gg \Gamma$ will hold. For such a practical situation, the experimentally observed lineshape can be approximated by

$$I_{expt}(\omega) = \exp\left(-k^2\sum_{j=1} a_j^2\frac{\hbar\eta}{mw_{2j}}\right)\frac{1}{2\pi} \times \int_{-\infty}^{\infty}\exp[-i(\omega-\omega_o)t - 1/2\Gamma \mid t \mid] \times \exp\left[-k^2\sum_{l\neq j} a_l^2\left(\frac{\hbar}{4mw_{2l}} - \frac{\eta\hbar}{mw_{2l}}\right)\exp(-\alpha_l \mid t \mid)\right]. \quad (13)$$

3.1 Translational and free-rotational diffusions

In the case of macro molecular systems, like proteins and polymers, the rotational diffusion may also influence the Mössbauer lineshape. The intermediate scattering function for a γ-ray with a wave-vector k is given by

$$G_{rot}(r,k,t) = \sum_{l=0}^{\infty}(2l+1)J_l^2(kr)e^{-l(l+1)}D_{rot}t \qquad (14)$$

where $J_l(x)$ is a Bessel function of order l and D_{rot} is the rotational diffusion constant. For the case in which rotational and translational diffusions are independent, the intermediate scattering function is given as

$$G_{tot}(r,k,t) = G_{rot}D(t). \qquad (15)$$

For a spherical particle of radius R with a homogenous density of the nuclei, the lineshape would be represented by

$$I(\omega) = \frac{3}{R^3}\int_o^R I(r,\omega)r^2dr \qquad (16)$$

where

$$\begin{aligned} I(r,\omega) &= \frac{1}{2\pi}\int_{-\infty}^{\infty}\exp[-i((\omega-\omega_o)t - \Gamma/2 \mid t \mid] \\ &\quad \times G_{tot}(r,k,t)dt \\ &= \sum_{l=0}^{\infty}\sum_{n=0}^{\infty}\frac{a_{nl}(r)\Gamma_{nl}/2\pi}{(\Gamma_{nl}/2)^2+(\omega-\omega_o)^2} \end{aligned} \qquad (17)$$

with

$$\Gamma_{nl}/2 = \Gamma/2 + n\alpha + l(l+1)D_{rot}$$

and

$$a_{nl} = \exp\left(-k^2\frac{\hbar\eta}{mw_2}\right)\frac{1}{n!}\left(\frac{\hbar k^2\eta}{mw_2} - \frac{\hbar k^2}{4mw_2}\right)^n (2l+l)J_l^2(kr).$$

The intensity of the spectrum is given as

$$\begin{aligned} A_{nl}\ R &= \frac{3}{R^3}\int_o^R a_{nl}(r)\ r^2\ dr \\ &= \frac{3}{2}\exp\left(-k^2\frac{\hbar\eta}{mw_2}\right)\frac{1}{n!}\left(\frac{\hbar k^2\eta}{mw_2} - \frac{\hbar k^2}{4mw_2}\right)^n (2l+1) \\ &\quad \times\left[J_l^2(kR) + J_{l-1}^2(kR) - \frac{(2l+1)}{kR}J_l(kR)J_{l-1}(kr)\right]. \end{aligned} \qquad (18)$$

It has been observed that the rotational diffusion affects Mössbauer by $\sim 20-30\%$. It has been experimentally observed in the spectra of iron magnetic particles located in bacteria [28].

3.2 Mean square displacement and linewidth

The mean square displacement (MSD) is given by

$$\langle x^2\rangle_q = (\hbar/mw_2)\eta \qquad (19)$$

where $\eta = [\exp\ (\beta\hbar w_2) - 1]^{-1}$. In the classical limit $\hbar \to 0$

$$\langle x^2\rangle = k_BT/mw_2^2. \qquad (20)$$

The diffusion constant D is given by

$$D = \hbar w_2\eta/m\lambda \qquad (21)$$

where λ is the damping constant. In the classical limit, $(\hbar \to 0)$, the relation between the MSD and diffusion constant can be written as

$$\langle x^2\rangle = (\lambda/w_2^2)D = D/\alpha. \qquad (22)$$

where $\alpha = w_2^2/\lambda$.

The effective MSD can be defined as

$$\langle x^2\rangle_e = mw_2\langle x^2\rangle/\hbar. \qquad (23)$$

The effective line width can be obtained [16] by equating

$$\begin{aligned} \frac{\Gamma_{eff}/2\pi}{(\Gamma_{eff}/2)^2+(\omega-\omega_o)^2} &= \frac{1}{\pi}\exp\{-k^2\langle x^2\rangle_q\} \\ &\quad \times\left[\frac{\Gamma/2}{((\Gamma/2)^2+(\omega-\omega_o)^2} + k^2\left(\frac{\hbar\eta}{mw_2} - \frac{\hbar}{4mw_2}\right)\right. \\ &\quad \left.\times\frac{(\Gamma/2+\alpha)/\pi}{(\Gamma/2+\alpha)^2+(\omega-\omega_o)^2}\right] \end{aligned} \qquad (24)$$

which, for $\omega = \omega_o$, gives the effective line-width Γ_{eff} as

$$\begin{aligned} \frac{1}{\Gamma_{eff}} &= \frac{1}{\pi}\exp[-k^2\langle x^2\rangle_q] \\ &\quad \times\left[\frac{2}{\Gamma} + \left(\frac{\hbar\eta}{mw_2} - \frac{\hbar}{4mw_2}\right)\frac{1}{(\Gamma/2+\alpha)}\right]. \end{aligned} \qquad (25)$$

In the classical limit, $\hbar \to 0$ mean square displacement (msd) is given as equation (22). The relation between msd and diffusion constant is given in equation (10). In the classical limit, $\hbar \to 0$ in equation (6), $I(\omega)$ reduces to

$$\begin{aligned} I(w) &= \exp(-k^2\langle x^2\rangle)\sum_{n=0}^{\infty}\frac{1}{n!}(k^2\langle x^2\rangle)^n \\ &\quad \times\frac{(\Gamma/2+n\alpha)/\pi}{(\Gamma/2+n\alpha)^2+(\omega-\omega_o)^2}. \end{aligned} \qquad (26)$$

The equation is the same as equation (5), obtained by Nowik *et al.* in the reference [16]. From the above equation, it is clear that the area under the curve remains constant because first two terms in equation (26) cancel out. Thus classical diffusion does not contribute to the recoil free factor and its temperature dependence is decided by the Debye model only. But in quantum case first two terms in equation (6) do not cancel out and quantum diffusion also

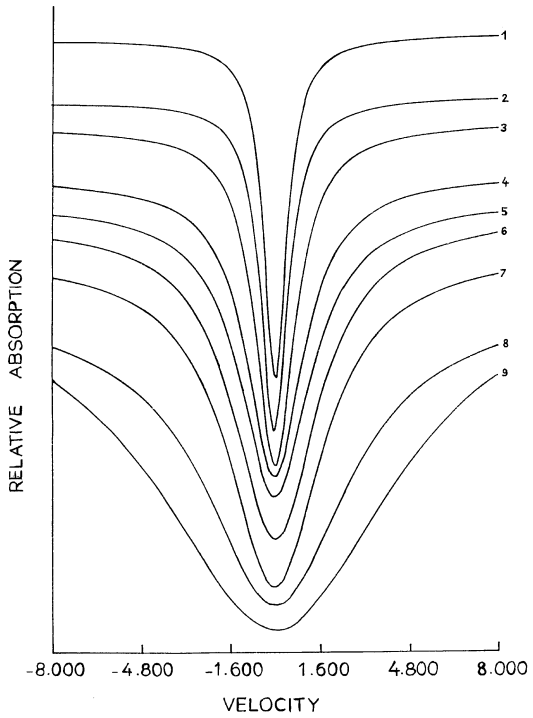

Fig. 1. Mössbauer Spectra of harmonically bound overdamped oscillators using equation (8). The plot is between $I(\omega)$ and velocity and by setting $w_2^2 = \alpha\lambda$. Curves marked from 1 to 9 have been obtained for different values of α. (1) $\alpha = 66$; (2) $\alpha = 65$; (3) $\alpha = 62$; (4) $\alpha = 58$; (5) $\alpha = 55$; (6) $\alpha = 50$; (7) $\alpha = 40$; (8) $\alpha = 10$; (9) $\alpha = 1$.

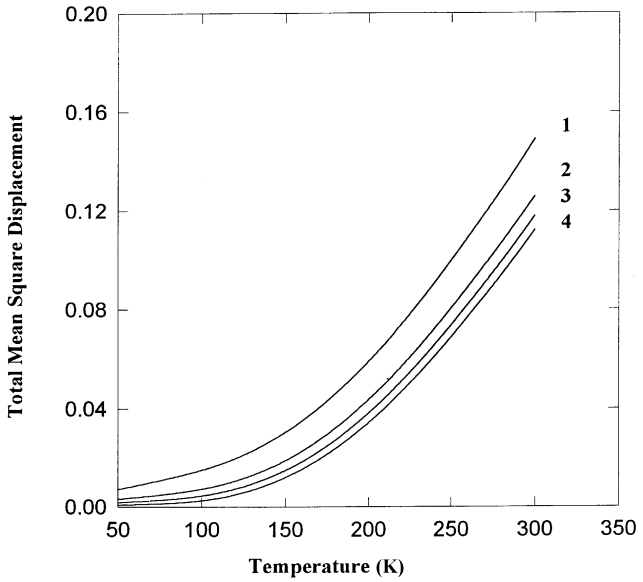

Fig. 2. This shows a plot of total mean square displacement for fixed value of $\hbar w/k = 700$ K, but for various values of Debye temperature (1) $\theta_D = 100$ K, (2) $\theta_D = 150$ K, (3) $\theta_D = 200$ K and (4) $\theta_D = 300$ K.

contributes to f factor apart from contribution due to Debye model. So classical models explain non-Lorentzian behaviour but cannot explain the temperature-dependence of msd and the linewidth. The quantum approach makes a difference when it comes to explaining the msd *versus* temperature behaviour and the linewidth *versus* temperature behaviour, apart from explaining the non-Lorentzian behaviour.

4 Discussion

The iron atom is known to be a vital part in life processes, as it is directly involved in storage of oxygen (haemoglobin and myoglobin) and electron transport (cytochrome and ferredoxins). It is also known that the interior of a protein molecule has two types of bonds. Along the amino-acid sequence, the backbone of the molecule is formed by strong covalent bonds, while the tertiary structure is the result of weak hydrogen-like bonds. A protein molecule has been visualised as a system, which is fluctuating over a large number of conformational substates. Molecules in different states have the same gross structure but differ in local configurations [24]. At local levels, there is a constant breaking and reforming of non-covalent bonds. The experiment of Austin *et al.* [25] implies that, although the different conformational substates have the same biological function but at different rates. At a low temperature, protein molecule is assumed to be frozen in one of the conformational substates of the distribution of the states. But at elevated temperature, the protein molecule may leave its conformational substate and enter a transition state with a certain degree of mobility before it gets trapped in another conformational substate. The motion in the transition state is identified with the diffusion of an overdamped Brownian quantum oscillator. The lineshape obtained for such an assumption is given by equation (6). The onset of the transition from one conformational substate to another also defines the characteristic temperature of the system. Below the characteristic temperature, all the conformational substates are frozen. Since the characteristic temperature is system dependent, each protein or polymeric system will have its own characteristic temperature, *e.g.*, for deoxy Mb it is 265 K. We have used equation (6) to compute the Mössbauer absorption spectrum. Figure 1 shows the computed Mössbauer spectra of harmonically bound quantum oscillators in Brownian motion as a function of the parameter $\alpha = w_2^2/\lambda$. It is observed that for an intermediate values of α, the spectra have a peculiar shape which is typical of some biological and polymeric systems. The total mean square displacement can be written as

$$\langle x^2\rangle_T = \langle x^2\rangle_V + \langle x^2\rangle_D \tag{27}$$

$\langle x^2\rangle_V$ is the contribution of vibrational degrees of freedom modelled in the present case by the Debye model. $\langle x^2\rangle_D$ is the contribution due to the diffusional motion. $\langle x^2\rangle_D$ has been modelled by considering different conformational states as quantum oscillators in the Brownian motion. Figure 2 shows a plot of mean square displacement for a fixed value of $\hbar w/k$ and for different values of the Debye temperature.

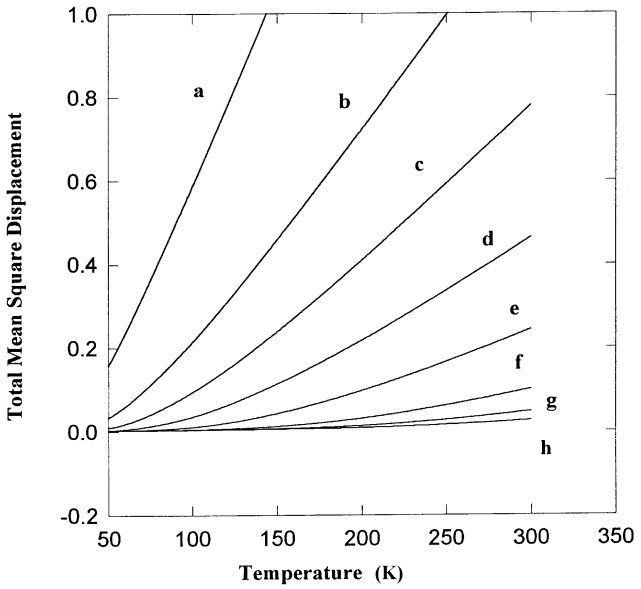

Fig. 3. This depicts a plot of total mean square displacement for fixed value of Debye temperature $\theta_D = 200$ K and for various values of $\hbar w/k$; (a) $\hbar w/k = 100$ K, (b) $\hbar w/k = 175$ K, (c) $\hbar w/k = 250$ K, (d) $\hbar w/k = 350$ K, (e) $\hbar w/k = 500$ K, (f) $\hbar w/k = 750$ K, (g) $\hbar w/k = 1000$ K, and (h) $\hbar w/k = 1250$ K.

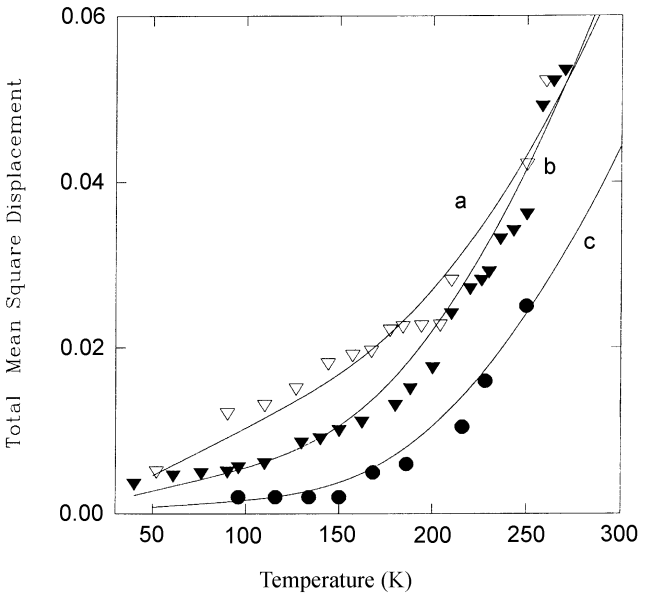

Fig. 4. Temperature dependence of total mean square displacement curves: the hollow traingles correspond to experimental data for Fe^{2+} bound to bacteriohodopsin [29] and fitted curve correponds to $hw/k = 920$ K for the Debye temperature equal to 120 K; the filled traingles correspond to the experimental data of freeze dried metmyoglobin samples [29] and the fitted curve corresponds to $hw/k = 980$ K for the Debye temperature equal to 300 K; and filled circles correspond to iron in chromatophes of Rhodospirillum Ruburum samples [29] and the fitted curve corresponds to $hw/k = 900$ K for the Debye temperature equal to 160 K.

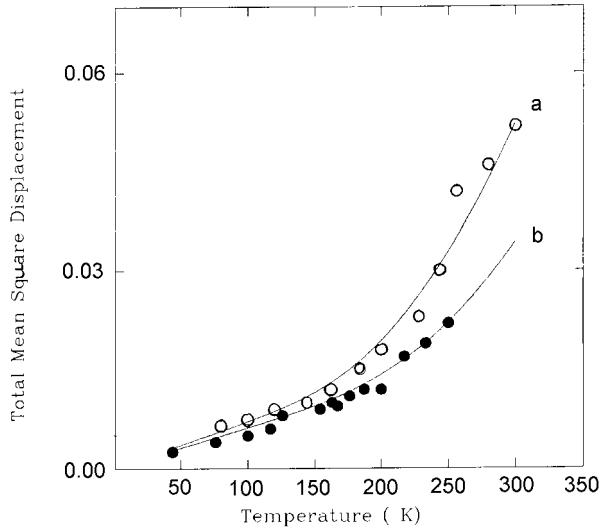

Fig. 5. Temperature dependence of total mean square displacement curves; the filled circle data corresponds to experimental data for Lechthin samples [29] and hollow circle data corresponds to Fe^{3+} bound to bacteiorhodospin samples [29]. Lechtin data has been fitted to curve corresponding to $hw/k = 1050$ K and Debye temperature equal to 140 K. Bacteiorhodospin data has been fitted to the curve corresponding to $hw/k = 1250$ K and Debye temperature equal to 150.

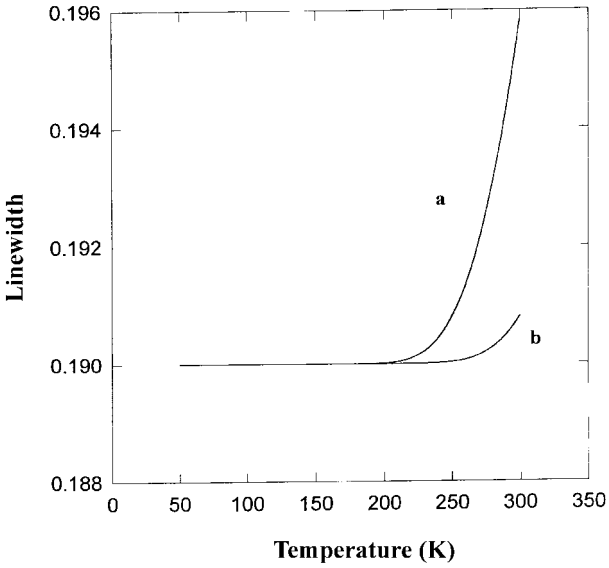

Fig. 6. Temperature dependence of linewidth for $\hbar w/k = 500$ K (a), 600 K (b).

From this figure, it is clear that greater the Debye temperature, smaller is the mean square displacement and *vice versa*. Also Debye temperature does not decide the shape of the curve. In contrast to this, Figure 3 depicts a plot of the mean square displacement for fixed values of the Debye temperature but for various values of $\hbar w/k$.

It is evident from Figure 3 that not only the values of the mean square displacement but also the shape of the curves is decided by the ratio $\hbar w/k$; it is clear that more

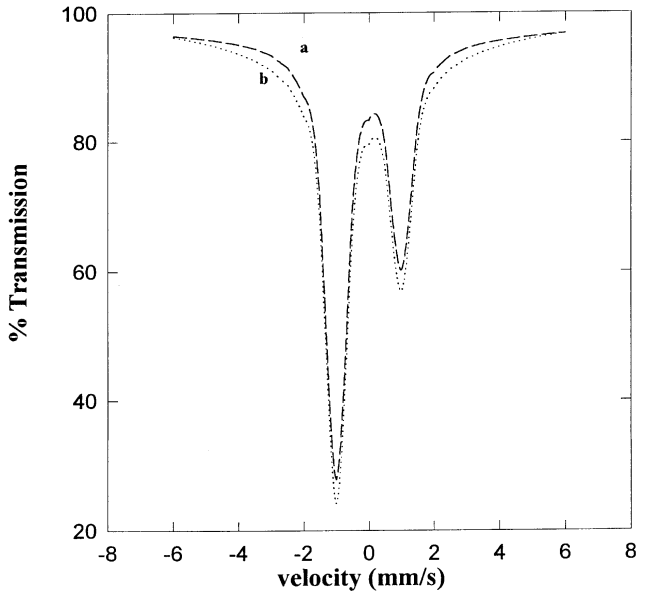

Fig. 7. Specta for harmonically bound overdamped Oscillator using equation (10) for $k^2\langle x^2\rangle_q = k^2\langle y^2\rangle_q = 2$. For curve (a) for $\alpha_x = 4$ and $\alpha_y = 40$ and for curve (b) $\alpha_x = 8$ and $\alpha_y = 8$.

the value of harmonic force constant w, less is the effect on the curvature of the figures, and *vice versa*. This is also demonstrated in Figures 4 and 5.

Figure 4 shows the plot of metamyoglobin, Fe^{2+} bound to bacteriorhodospin and Rhodospirillim Rubrum samples. Figure 5 shows Fe^{3+} in bacteriorhodospin and Lecthin samples. Figure 6 depicts the temperature dependence of the linewidth.

In Figure 7, the Mössbauer spectra of harmonically-bound particles, acted upon by axially symmetric anisotropic damping forces, is depicted. The asymmetry in the spectra is observed even for α values being equivalent for two lines as is clear in Figure 7. The most important contribution of the present picture is (i) temperature dependence of msd (mean square displacement) (ii) temperature dependence of the linewidth can be explained with out taking into account additional degrees of freedom.

I am very thankful of anonymous referees for turning my attention towards few additional references and also for their critical assessment which helped in improvement of this paper. I am also thankful of my colleague Dr C.L. Kaul for his help in solving some equations.

References

1. S.G. Cohen, E.R. Bauminger, I. Nowik, S. Ofer, J. Yariv, Phys. Rev. Lett. **46**, (1981) 1244.
2. R.R. Bauminger, S.G. Cohen, I. Nowik, J. Yariv ICAME-1981, edited by V.G. Bhide INSA proceedings (New Delhi, 1982).
3. K.H. Mayo, F. Parak, R.L. Mössbauer, Phys. Lett. A **82**, 468 (1981).
4. E.R. Bauminger, S.G. Cohen, I. Nowik, S. Ofer, J. Yariv Proc. Nat. Acad. U.S.A. **80**, (1983) 763.
5. E.R. Bauminger, S.G. Cohen, E. Giberman, I. Nowik, S. Ofer, J. Yariv, M.W. Werber and Mevarech , J. Phys. Colloq. France **37**, C6-227 (1976).
6. S.G. Cohen, E.R. Bauminger, I. Nowik, S. Ofer, J. Yariv, in *Biomolecular Stereodynamics* (Adenine, 1981), Vol. 2, p. 229.
7. F. Parak, M. Fisher, J. Heidemer, M. Engelhard, K.D. Kohl, B. Hess, H. Formanek, Hyperfine Interaction **58**, 2381 (1990).
8. E.R. Bauminger, S.G. Cohen, S. Ofer, U. Bachrach Biochim. Biophys. Acta **7200**, 133 (1982).
9. C. Heither-Wirguin, E.R. Bauminger, A. Levy, F. Labensky, De Kanter, S. Ofer, Polymer **21**, 1324 (1980).
10. K. Wuthrick, *NMR of proteins and nuclei acids* (Wiley, New York, 1986).
11. S. Cusack, J. Smith, J. Pinney, M. Karplus, J. Trewhella, Physica B **136**, 256 (1986).
12. Yu.F. Krupyanskii, V.I. Goldauskii, G.U. Nienhaus, F. Parak, Hyperfine Interaction **53**, 59 (1990).
13. I.V. Kurinov, Yu.F. Krupyanskii, A.R. Panchenko, I.P. Sozdalev, I. Uporov, K.V. Shaitan, A.B. Rubin, V.I. Goldanskii, Hyperfine Interaction **58**, 2355 (1990).
14. F. Parak, E.W. Knapp, D. Kucheida, J. Mol. Bio. **61**, 177 (1981).
15. I. Nowik, E.R. Bauminger, S.G. Cohen, S. Ofer, Phys. Rev. Lett. **50**, 1528 (1983).
16. I. Nowik, E.R. Bauminger, S.G. Cohen, S. Ofer, Phys. Rev. A **31**, 2291 (1985).
17. H. Keller, P.G. Debrunner, Phys. Rev. Lett. **45**, 68 (1980).
18. E.W. Knapp, S.F. Fisher, F. Parak, J. Chem. Phys. **78**, 4701 (1983).
19. E.W. Knapp, F. Parak, S.F. Fisher, J. Phys. Chem. **86**, 5042 (1982).
20. M.C. Wang, G.E. Uhlenbeck, Rev. Mod. Phys. **17**, 323 (1945).
21. G.S. Agarwal, Phys. Rev A **4**, 739 (1971).
22. S. Dattagupta, Phys. Rev. A **30**, 1525 (1984).
23. S. Dattagupta, G.F. Reiter, Phys. Rev. A **31**, 1034 (1985).
24. H. Frauenfelder, G.A. Petsko, D. Tsernoglou, Nature (London) **280**, 558 (1979).
25. R.H. Austin, K.W. Besson, L. Eisentein, H. Frauenfelder, I.C. Gunsalus, Biochem. **14**, 5355 (1975).
26. A. Kumar, Phys. Lett. A **154**, 461 (1991).
27. A.M. Afanseev, V.E. Sedov, Phys. Stat. Sol. B **131**, 299 (1985).
28. S. Ofer, I. Nowik, E.R. Bauminger, G.C. Papafthymion, R.B. Frenkel, R.B. Blakemore, Biophys. J. **46**, 57 (1984).
29. F. Parak, J. Heidemeier, G.U. Nienhaus, Hyperfine Interactions **40**, 147 (1988).
30. F. Parak, E.N. Prolov, R.L. Mössbauer, V.I. Goldanskii, J. Mol. Biology **145**, 147 (1981).
31. K.S. Singwi, A.Sjolander, Phys. Rev. **120**, 1093 (1960).
32. G.E. Ulhenbeck, L.S. Orneistein, Phys. Rev. **36**, 823 (1930).
33. L. Gunther, J. Zitkova-wilcox, J. Phys. France **35**, C6-519 (1974).
34. L. Gunther, J. Zitkova-wilcox, J. Stat. Phys. **12**, 205 (1975).